

10. SITE 1159¹

Shipboard Scientific Party²

PRINCIPAL RESULTS

Site 1159 is located in Zone A, 240 km southeast of Site 1158, close to or outside the eastern margin of the depth anomaly, ~160 km east of the ~127°E fracture zone. The seafloor magnetic age is ~14 Ma. This is the youngest seafloor drilled during Leg 187 and the southernmost site along a north-south transect designed to locate possible occurrences of Indian-type mantle beneath western Zone A. The site is located in a very small sediment-filled basin in an area dominated by axis-parallel seafloor fabric with little or no sediment cover.

Hole 1159A was spudded in 4504 m water depth and was washed through ~145 m of sediment. We recovered a single wash barrel with 4.5 m of drilling-disturbed carbonate ooze and three pieces of aphyric basalt in the lowermost part. Rotary drilling continued 28 m into basement, recovering 7.96 m (28.7%) of aphyric basalt and a few pieces of hyaloclastite breccia with interstitial sediment. The basalts were assigned to a single unit of moderately altered aphyric pillow lava with alteration halos along piece margins and veins.

Two basalt glasses were analyzed for major and trace elements by inductively coupled plasma-atomic emission spectrometry (ICP-AES), and two whole-rock powders were analyzed by both X-ray fluorescence (XRF) and ICP-AES. The glasses are moderately evolved with 7.7–8.0 wt% MgO, and their compositions are similar in most respects to 0- to 7-Ma lavas from Segment A3, east of the AAD. The whole rocks range in MgO from 6.9 to 7.3 wt%, differing from the glasses by a smaller margin than at most of our earlier sites. As at the other sites, this difference appears to be mainly attributable to alteration. The Ba and Zr contents of the glasses indicate a Pacific-type mantle reservoir beneath this site. This is the fourth Pacific site of the five sites drilled in western Zone A, reinforcing the conclusion that the Indian/Pacific mantle boundary is closely associated with the eastern margin of the depth anomaly.

¹Examples of how to reference the whole or part of this volume.

²Shipboard Scientific Party addresses.

OPERATIONS

Transit to Site 1159

The eighth site of Leg 187 is 133 nmi southeast of Site 1158. We conducted a 3.5-kHz and single-channel seismic (SCS) survey at ~6 kt during the entire transit. The purpose of this survey was to locate additional drilling targets on a line between Sites 1158 and 1159 (see “Site Geophysics,” p. 4).

Hole 1159A

We deployed a positioning beacon on the prospectus Global Positioning System (GPS) coordinates at 2208 hr on 18 December. The precision depth recorder (PDR) water depth for this site is 4515.4 m below the rig floor. The nine-collar bottom-hole assembly (BHA) used on the other sites was reassembled, using the same C-7 four-cone rotary bit from the previous site. We began washing through the sediment column at 0645 hr on 18 December and reached basement at 145.6 meters below seafloor (mbsf) in just over 2 hr. After recovering the wash barrel (Core 187-1159A-1W), we advanced by coring from 145.6 to 173.3 mbsf (Cores 187-1159A-2R through 7R; see Table T1). Hole conditions deteriorated rapidly while we were drilling Core 187-1159A-7R, as indicated by a sudden increase in penetration from ~2 m/hr to >10 m/hr. We abandoned the hole when we were unable to regain our previous sub-bottom depth because of fill in the hole. Core 187-1159A-8G was recovered but represents no new penetration. The rocks recovered in this core do not appear to have been cut by the bit, and we interpret them as rubble fallen into the hole and collected during the hole cleaning attempt. A tracer of fluorescent microspheres was deployed on Core 187-1159A-2R. The drill string cleared the seafloor at 1115 hr and the rotary table at 1945 on 20 December, ending operations at this site.

IGNEOUS PETROLOGY

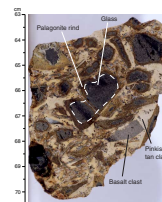
Hole 1159A was rotary cored into igneous basement from 145.6 to 173.3 mbsf. We recovered 7.96 m of core, equal to 28.7% recovery (Sections 187-1159A-2R-1 through 7R-2). Following hole collapse after Core 187-1159A-7R, we attempted to resume coring and recovered 0.24 m of core (Section 8G-1) with no further penetration.

From this hole we recovered a single unit of medium to dark gray aphyric basalt interpreted as intact pillow lava, based on uniform lithology and the high percentage of pieces with arcuate chilled margins and/or glass rinds. Two pieces of hyaloclastite breccia—consisting of angular to subrounded glass/palagonite clasts (1–3 cm in size) in a pinkish tan clay matrix (Fig. F1)—were recovered, one in Section 187-1159A-6R-2 and one in Section 7R-1. We interpret these pieces as accumulations of glass that spalled off pillows and collected with clay-rich sediment in interpillow spaces.

Overall, the basalt is slightly to moderately altered (see “Alteration,” p. 3). Phenocrysts include <1% equant to euhedral olivine (up to 1 mm in size) and <1% prismatic plagioclase (up to 2 mm in size). Many pieces from this unit display chilled margins, with 12% of the pieces having an outer glassy/palagonite rind (as thick as 2 cm but usually ~1 mm thick) and 33% of the pieces having a spherulitic margin that

T1. Coring summary, Site 1159, p. 27.

F1. Hyaloclastite breccia, p. 7.



grades from a dark gray to black (in hand specimen) outer band of small, 3- to 4- μm cryptocrystalline quench crystals to a tan-brown band of larger (~1 to 2 mm in diameter) coalesced plagioclase quench spherulites (Fig. F2).

As seen in thin section, the microcrystalline groundmass of pillow interiors is dominated by plagioclase sheaf quench textures (~35%–40%), with 10%–15% equant to elongated quenched olivines <0.2 mm in size (Fig. F3). The remaining 45%–55% is black mesostasis. The basalt contains 1%–2% spherical vesicles up to 1.5 mm in diameter that are variably lined, partially or completely filled with green clay (smectite?), yellow-tan clay, cryptocrystalline quartz, Fe oxyhydroxide, or Mn oxide.

ALTERATION

Basalts recovered from Hole 1159A represent a single lithologic unit that is slightly to moderately altered by low-temperature reactions. The alteration is strongest within oxidation halos along fractures, veins, and outer edges of pieces, in areas with vugs, and within the inner part of chilled margins that have large coalesced spherulites. The alteration elsewhere is slight but commonly pervasive.

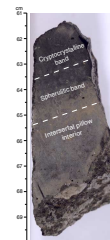
Throughout the hole, alteration halos (1–7 mm wide) are present along thin (<1 mm) fractures that range from unfilled to silica and/or clay lined. Except for Sections 187-1159A-7R-1 and 8G-1, thin (as thick as 1 mm), branching veins that are lined with Fe oxyhydroxide \pm Mn oxide and filled with orange-red to yellow and green clay and/or silica are also common. In veins where both silica and clay are present, silica cuts through the clay, indicating that silica infilling was the last stage in vein formation (Figs. F4, F5). Around uncut outer surfaces of pieces, oxidation halos vary in width from 1 to 15 mm, with an average of 5 mm. These surfaces are commonly coated with silica and clay and/or Mn oxide and probably represent fracture and/or vein surfaces.

Fracture plus vein density averages 19.8/m (ranging from 5.0 to 30.8/m), and vein density averages 3.9/m (ranging from 0 to 7.7/m). The calculated volume percent of veins averages 0.11 vol% (ranging from 0 to 0.23 vol%).

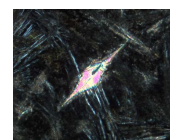
In Sections 187-1159A-2R-1 (Piece 8) and 5R-1 (Piece 2), vugs (as long as 1.7 cm and as wide as 5 mm) are lined with Fe oxyhydroxide and Mn oxide and are partially to completely filled with silica or clay of various colors (red, brown, or yellowish white to green). In Section 2R-1 (Piece 8), the vugs are surrounded by 3–4 mm oxidation rims (Fig. F6). In Section 187-1159A-5R-1 (Piece 2), however, no distinct oxidation rims are developed around the vugs, but a larger area surrounding the vugs is altered to a higher degree than outside halos in other pieces (Fig. F7). In most pieces throughout the core, vesicles are unfilled or lined to completely filled with Fe oxyhydroxide \pm Mn oxide \pm orange-brown or yellowish white to green clay \pm silica (Figs. F8, F9).

Symmetrical rims of yellow-brown altered glass (palagonite) are developed along a network of silica-filled veins within one piece of shiny black glass (Section 187-1159A-4R-1 [Piece 6]). A 3- to 5-mm-wide fracture cutting through the piece is partially filled with quartz-cemented, small altered glass fragments (Fig. F10). Within the inner part of chilled margins, a 1- to 2-cm layer of large coalesced spherulites is commonly highlighted because the surrounding groundmass has been replaced by a light brown clay. The alteration is usually connected to fractures that are parallel to or crosscut the spherulitic layer (e.g., Fig. F11). The outer

F2. Spherulitic chilled margin, p. 8.



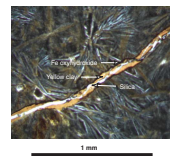
F3. Lantern-shaped olivine with quench crystal extensions, p. 9.



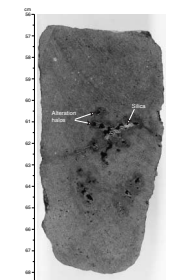
F4. Silica vein crosscutting Fe oxyhydroxide- and clay-filled veins, p. 10.



F5. Vein lined with Fe oxyhydroxide, filled with orange clay, and crosscut by later silica, p. 11.



F6. Alteration halos around vugs, p. 12.



part of the partially crystallized quenched margin shows, however, little sign of alteration along the fractures. This may indicate that the alteration is controlled by different quench textures. Glass fragments in pieces of clay-cemented hyaloclastite (Sections 187-1159A-6R-2 and 7R-1) are partially to completely replaced by 0.5- to 5-mm-thick palagonite rims around the edges (Fig. F12).

Within the oxidation halos and within areas with vugs, 20%–100% of the groundmass is generally replaced by Fe oxyhydroxide and/or red-brown to yellowish green clay. Elsewhere the groundmass shows a patchy replacement from 1% to 20% by Fe oxyhydroxide and/or yellowish to green clay. In many cases the patches are forming thin, arcuate, wavy patterns, suggesting that these may be outlining quench crystallization textures. When present, phenocrysts of olivine are partially to completely replaced by Fe oxyhydroxide, but plagioclase is unaltered.

MICROBIOLOGY

At Site 1159, four rock samples were collected as soon as the core liners were split to characterize the subsurface microbial community (Table T2). One sample is a breccia fragment (Sample 187-1159A-6R-2 [Piece 11, 73–75 cm]), and three are pillow basalt fragments composed of partially altered glass rinds and crystalline basalt interiors (Samples 187-1159A-2R-1 [Piece 7, 53–56 cm], 3R-1 [Piece 10A, 62–65 cm], and 7R-1 [Piece 25, 131–134 cm]). To sterilize them, the outer surfaces of the rock samples were quickly flamed with an acetylene torch, and enrichment cultures and samples for DNA analysis and electron microscope studies were prepared (see “Igneous Rocks,” p. 7, in “Microbiology” in the “Explanatory Notes” chapter).

Fluorescent microsphere tests were carried out for one rock core to evaluate the extent of contamination caused by drilling fluid (see “Tracer Test,” p. 9, in “Microbiology” in the “Explanatory Notes” chapter and Table T2). Pieces of rock were rinsed in nanopure water, the collected water was filtered, and the filter was examined for the presence of microspheres under a fluorescence microscope. Thin sections were used to examine the extent of contamination inside the sample. Microspheres were observed on the filter but not in the thin sections; this may be because the thin sections were almost fracture free.

SITE GEOPHYSICS

Site 1159 was located based on 1996 SCS site survey data and confirmed by a short 3.5-kHz PDR and SCS presite survey from the *JOIDES Resolution* (JR). Onboard instrumentation included a precision echo sounder, gyrocompass, seismic system, and GPS receivers.

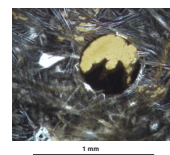
Seismic Reflection Profiling

Site selection for Site 1159 was based on a SCS survey conducted during the *R/V Melville* cruise Boomerang 5 in 1996. A 22.1-hr SCS and 3.5-kHz PDR survey was conducted all the way from Site 1158 to Site 1159 (JR SCS line S7; see Fig. F13) to locate potential new drill sites. This survey line terminated soon after crossing the prospectus site AAD-2b. The ship’s average speed was 5.8 kt, and the course was 160° when the SCS

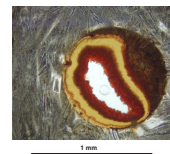
F7. Moderately altered basalt with vugs, p. 13.



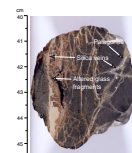
F8. Vesicle filled with yellow clay and Mn oxide, p. 14.



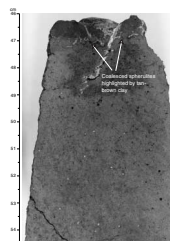
F9. Vesicle filled with yellow clay and Fe oxyhydroxide, p. 15.



F10. Crosscutting silica veins in glassy pillow margin, p. 16.



F11. Quartz-filled fracture cross-cutting a chilled margin, p. 17.



F12. Clay-cemented hyaloclastite, p. 18.



survey approached Site 1159 (AAD-2b). The water gun was triggered at shot intervals of 12 s, equivalent to ~36 m at 5.8 kt. Data acquisition and processing parameters are described in “Underway Geophysics,” p. 10, in the “Explanatory Notes” chapter. We marked the position of Site 1159 near seismic shotpoint 6425 of line S7, where the water depth is 4504.2 m (see Fig. F14). Although there are significant out-of-plane reflectors, the sediment cover (Fig. F14) extends from 6.2 to 6.35 s in two-way travelttime, equivalent to at least 150 m of sediment. Hole 1159 was drilled through 145.6 m of sediment before basement was reached.

Three new proposed sites (AAD-38a, 39a, 40a) were located near shotpoints 1200, 2425, and 5050 (Figs. F15, F16, F17). Sediment thicknesses estimated from the SCS profile are 150, 280, and 280 m, respectively. Sites AAD-38a and 39a were subsequently drilled as Sites 1161 and 1162.

SEDIMENTS

We recovered a single wash barrel between 0.0 and 145.6 mbsf from Hole 1159A. All four sections (187-1159A-1W-1 through 1W-CC) contain carbonate ooze. The upper 47 cm of Section 187-1159A-1W-1 is fine- to medium-sand-sized globular calcareous microfossils in a slurry of very light brown clay. The remaining core is severely drilling disturbed, mainly very light brown, carbonate-rich clay. The lowermost 23 cm of Section 187-1159A-1W-3 and the core-catcher (CC) section contain densely packed, very light brown calcareous clay with several subtle color changes in varying shades of slightly darker brown clay. Rarely, there are centimeter-thick intervals in which concentrations of abundant microfossils are present, but the contacts of these layers are disrupted by drilling. Three pieces of aphyric basalt were recovered in the lowermost part of Section 187-1159A-1W-CC.

GEOCHEMISTRY

Introduction

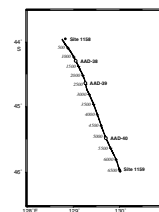
Site 1159 basalts were recovered from a single hole that yielded samples of ~14-Ma crust formed within Zone A of the Southeast Indian Ridge. Two whole-rock powders were analyzed for major and trace elements by XRF and ICP-AES, and two samples of fresh basalt glass chips were analyzed by ICP-AES (Table T3). Relative to the XRF analyses, Al₂O₃, Fe₂O₃, MgO, and Na₂O contents are higher and Ni and Cr are lower for the ICP-AES analyses. All other elemental analyses are in good agreement between both the XRF and ICP-AES analyses.

Hole 1159A

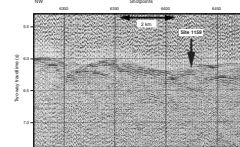
From Hole 1159A we recovered samples from a single lithologic unit of aphyric pillow basalt (see “Igneous Petrology,” p. 2). The glass samples from this site contain ~1 wt% more SiO₂, ~0.5 wt% more MgO, ~0.2 wt% less K₂O, and 3 to ~4 ppm less Ba than the whole-rock samples (Table T3). All other elements are similar in whole-rock and glass samples. The slight compositional differences in CaO and Al₂O₃ between the whole-rock and the glass samples could be explained by fractional crys-

T2. Rock samples for cultures, DNA analysis, SEM/TEM, and contamination studies, p. 28.

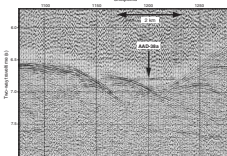
F13. Track chart of the JR SCS survey line S7, p. 19.



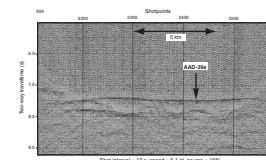
F14. SCS profile from line S7, shotpoints 6270 to 6480, p. 20.



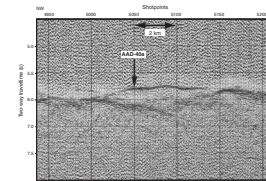
F15. SCS profile from line S7, shotpoints 1025 to 1285, p. 21.



F16. SCS profile from line S7, shotpoints 2110 to 2580, p. 22.



F17. SCS profile from line S7, shotpoints 4935 to 5215, p. 23.



T3. Compositions of basalts from Site 1159, p. 29.

tallization of plagioclase or by crystal sorting, as they parallel low-pressure crystal fractionation trends of axial Zone A lavas (Fig. F18). The whole-rock–glass variations on TiO_2 and Fe_2O_3 vs. MgO plots, however, are oblique to these fractionation trends and are therefore inconsistent with low-pressure crystal fractionation. These observations are similar to previous sites, suggesting that alteration is the dominant cause of the low- MgO whole-rock compositions.

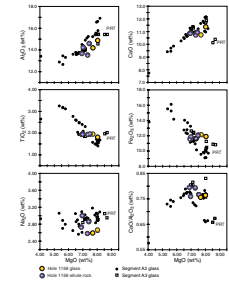
Temporal Variations

In Figures F18 and F19, Site 1159 glasses are compared to 0- to 7-Ma Zone A lavas from Segments A2 and A3. Site 1159 glasses have similar compositions to 0- to 7-Ma Zone A lavas, although Y contents are slightly higher and Sr slightly lower at the same MgO content. We note that Fe_2O_3 is significantly higher (~2 wt%) and Na_2O is lower than the 0- to 7-Ma Zone A lavas, which could suggest slightly deeper melting conditions. However, higher degrees of melting are not supported by $\text{CaO}/\text{Al}_2\text{O}_3$. Therefore, the general similarity between Site 1159 and Segments A2 and A3 lavas suggests a comparable mantle source composition and comparable mantle melting conditions. The low Sr, Ba, and Na_2O also indicate that Site 1159 lavas erupted along a section of the spreading axis away from propagating rift tips.

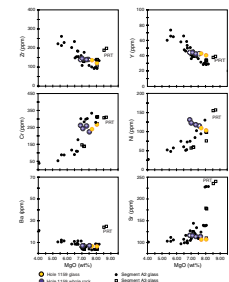
Mantle Domain

Site 1159 samples plot clearly in the Pacific field on the Zr/Ba vs. Ba diagram (Fig. F20A), suggesting a Pacific-type mantle source existed in this portion of Zone A at ~14 Ma. The $\text{Na}_2\text{O}/\text{TiO}_2$ vs. MgO characteristics for Site 1159 basalts are also consistent with a Pacific-type mantle source (Fig. F20B).

F18. Major element compositions of Site 1159 basalts vs. MgO , p. 24.



F19. Trace element compositions of Site 1159 basalts vs. MgO , p. 25.



F20. Variations of Zr/Ba vs. Ba and $\text{Na}_2\text{O}/\text{TiO}_2$ vs. MgO for Site 1159 basalt glass and whole-rock samples, p. 26.

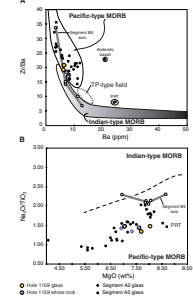


Figure F1. Photograph of interval 187-1159A-6R-2, 63–71 cm, showing hyaloclastite breccia. The smaller elongate clasts are subrounded to angular glass fragments with palagonite rims. The matrix is pinkish tan clay.

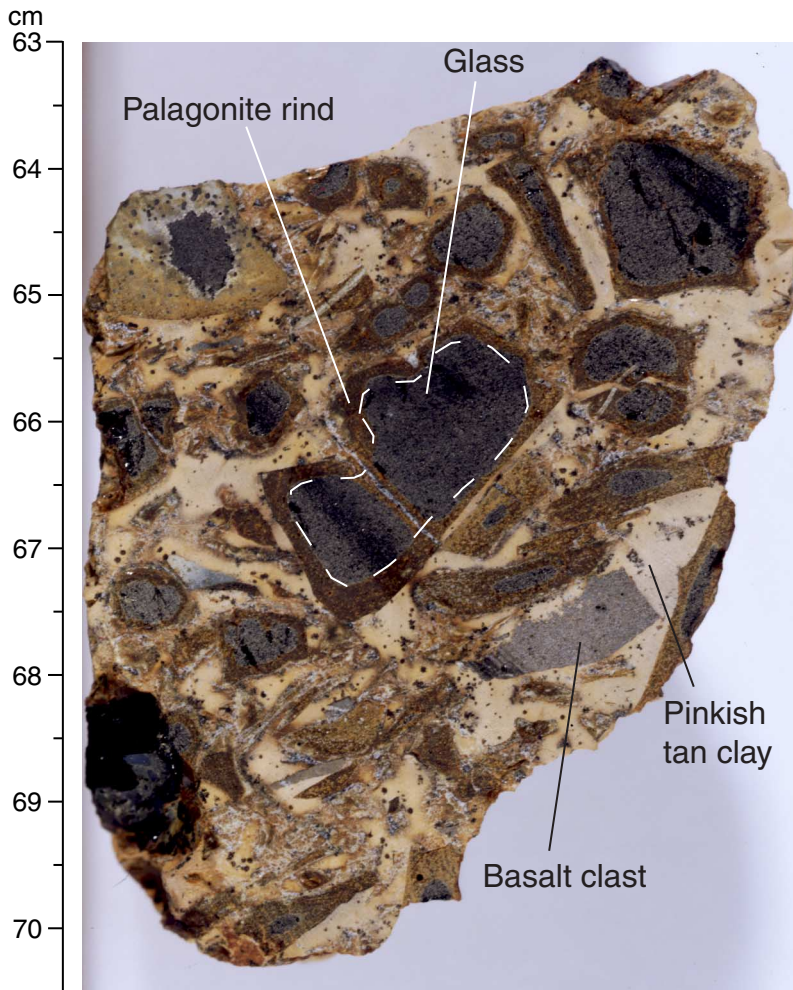


Figure F2. Photograph of interval 187-1159A-3R-1, 61–70 cm, showing a chilled margin grading from a dark gray outer zone of cryptocrystalline quench crystals to an inner tan-brown zone of coalesced plagioclase spherulites.

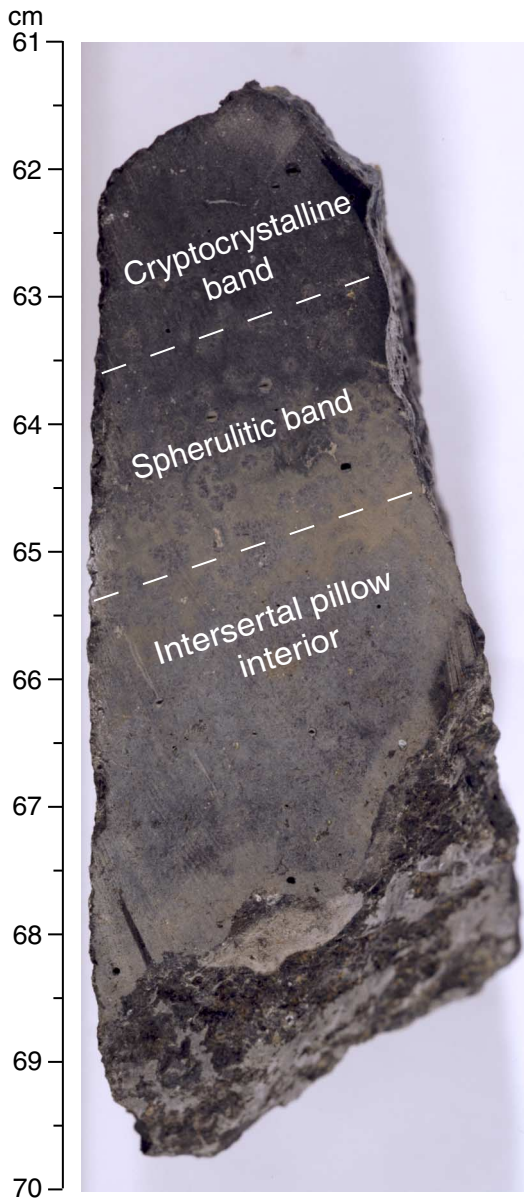
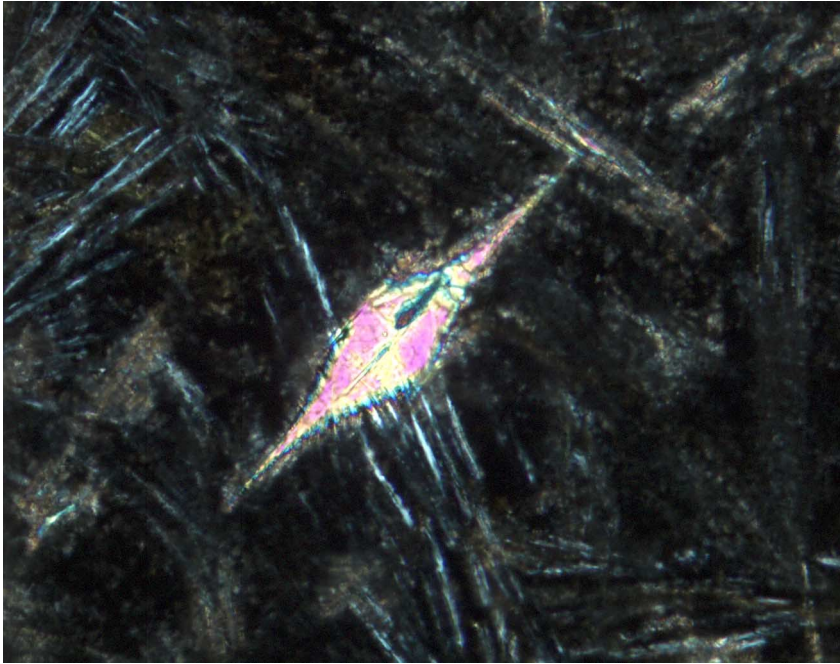


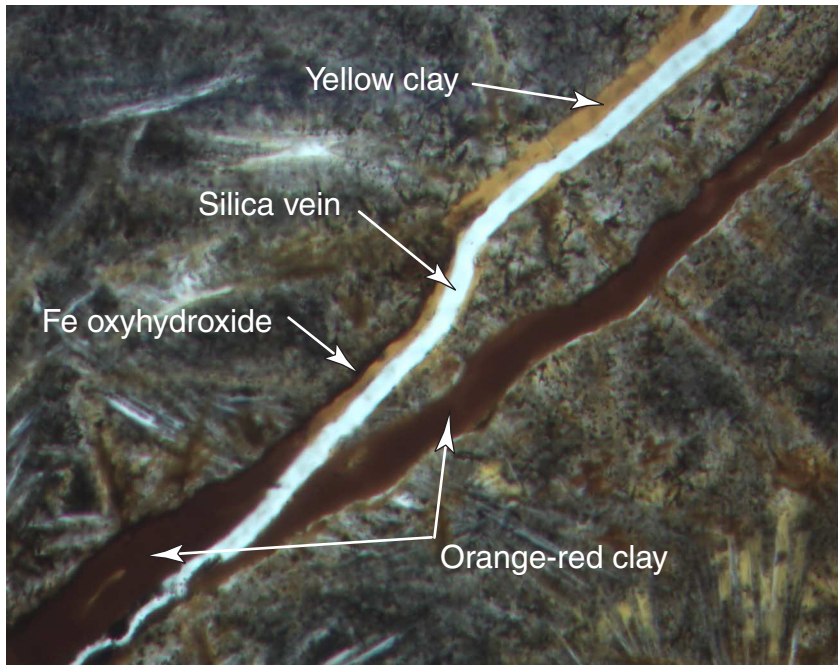
Figure F3. Photomicrograph, with crossed polars, of Sample 187-1159A-2R-1, 20–24 cm, showing a lantern-shaped olivine with quench crystal extensions. See “Site 1159 Thin Sections,” p. 13.



0.5 mm



Figure F4. Photomicrograph in plane polarized light of Sample 187-1159A-5R-2, 97–101 cm (see “Site 1159 Thin Sections,” p. 16), showing silica vein crosscutting Fe oxyhydroxide- and clay-filled veins.



0.5 mm

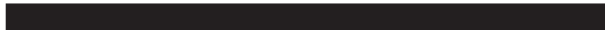
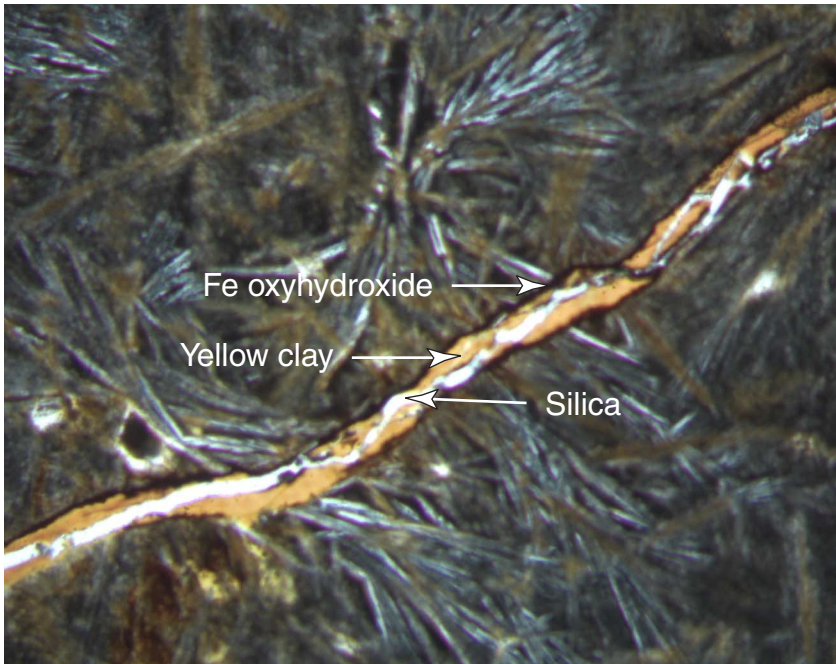


Figure F5. Photomicrograph in plane polarized light of Sample 187-1159A-5R-2, 97–101 cm (see “[Site 1159 Thin Sections](#),” p. 16), showing a vein lined with Fe oxyhydroxide, filled with orange clay, and crosscut by later silica.



1 mm



Figure F6. Photograph of interval 187-1159A-2R-1, 56–68 cm, showing alteration halos around vugs, which are now partially filled with Mn oxide and silica.

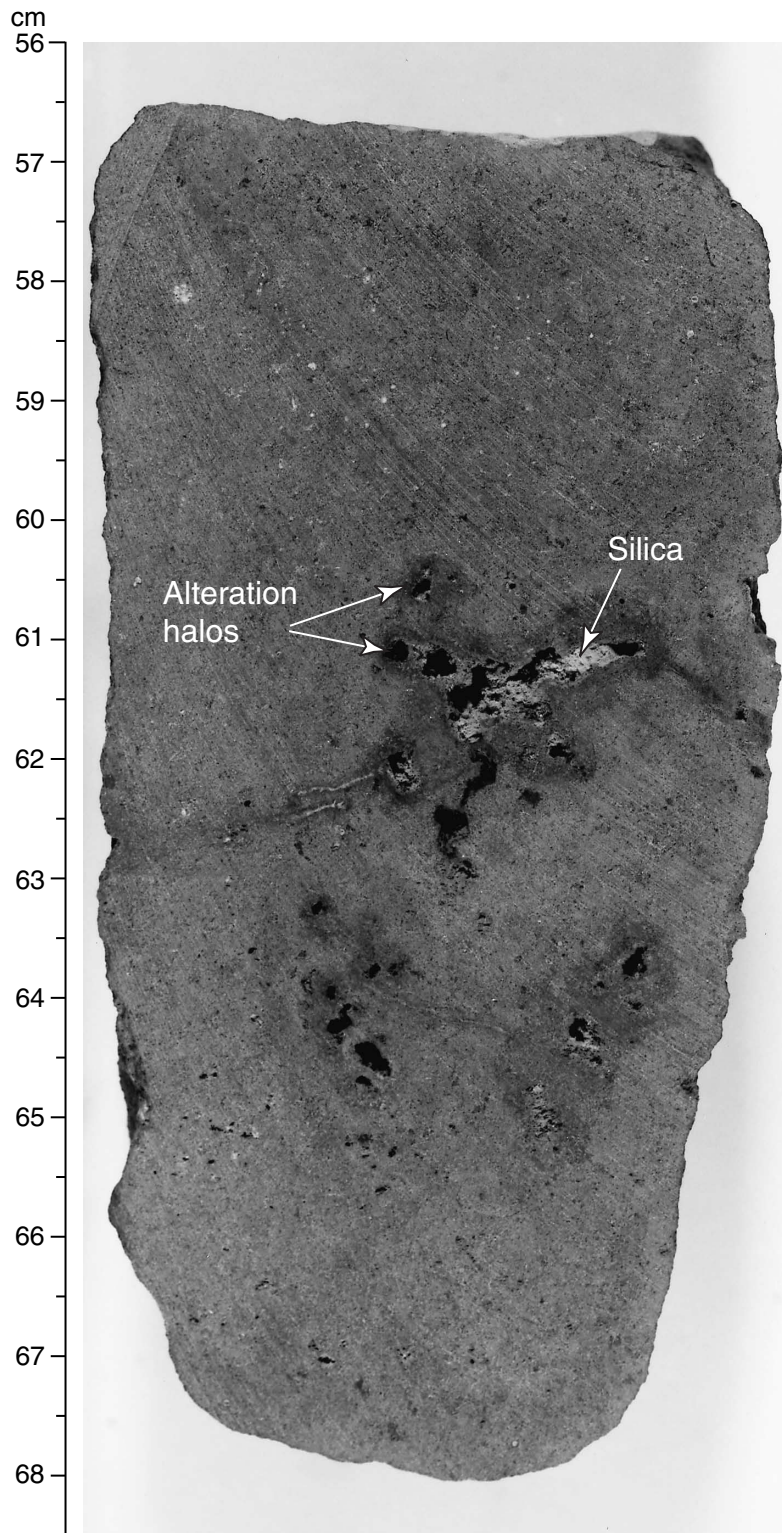


Figure F7. Photograph of interval 187-1159A-5R-1, 6–20 cm, showing a moderately altered basalt with vugs lined with Fe oxyhydroxide and/or Mn oxide and partially to completely filled with clay and/or silica.

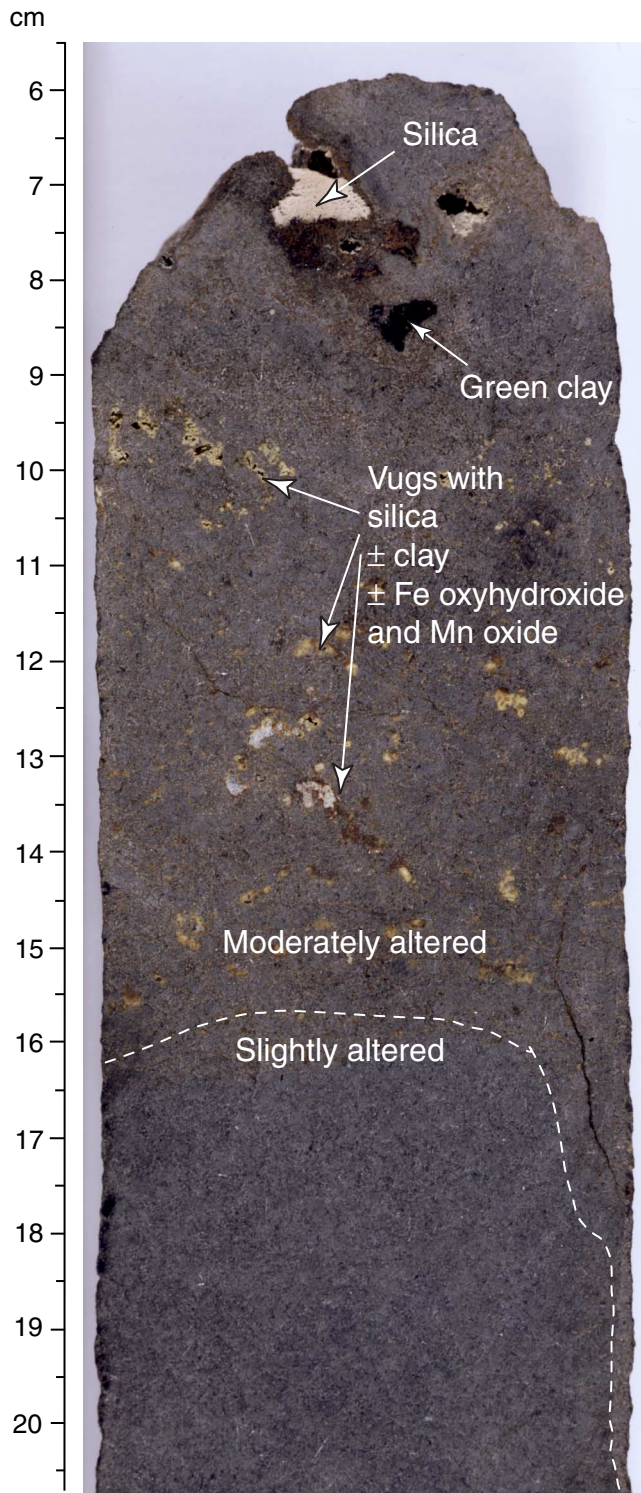
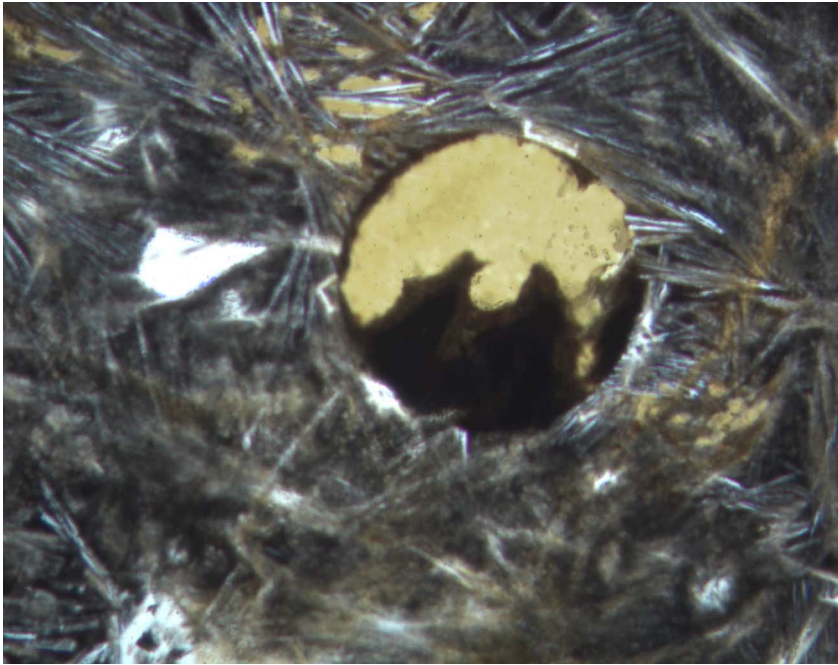


Figure F8. Photomicrograph in plane polarized light of Sample 187-1159A-5R-2, 97–101 cm (see “[Site 1159 Thin Sections](#),” p. 16), showing vesicle filled with yellow clay and Mn oxide. Mesostasis between quench crystals is partly replaced by yellow clay.



1 mm



Figure F9. Photomicrograph in plane polarized light of Sample 187-1159A-2R-1, 20–24 cm (see “[Site 1159 Thin Sections](#),” p. 13), showing a vesicle filled with yellow clay and Fe oxyhydroxide.



1 mm

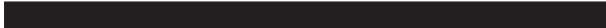


Figure F10. Photograph of interval 187-1159A-4R-1, 40–45 cm, showing a network of crosscutting silica veins in a glassy pillow margin. Parallel to the left side, 3- to 5-mm-wide fractures are filled with small, altered, quartz-cemented glass fragments.

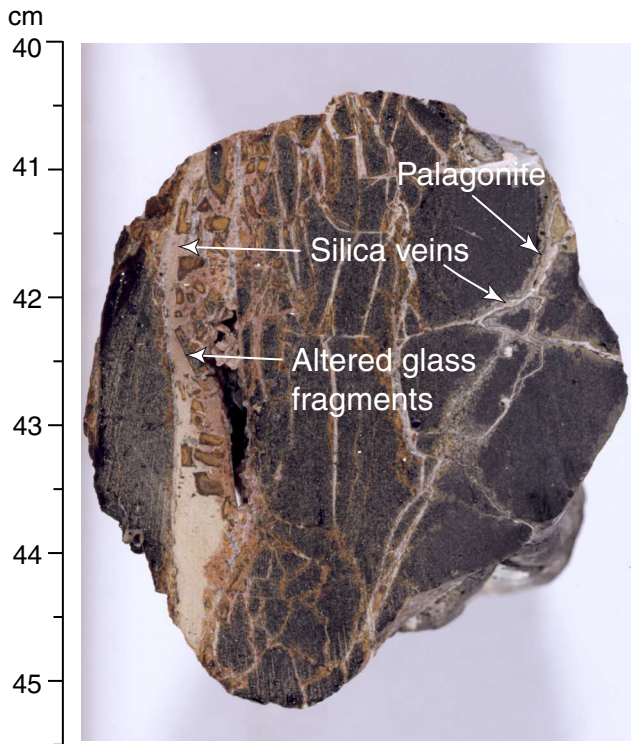


Figure F11. Photograph of interval 187-1159A-4R-1, 46–54 cm, showing a quartz-filled fracture crosscutting a chilled margin. Large coalesced spherulites are highlighted by light brown clay alteration.

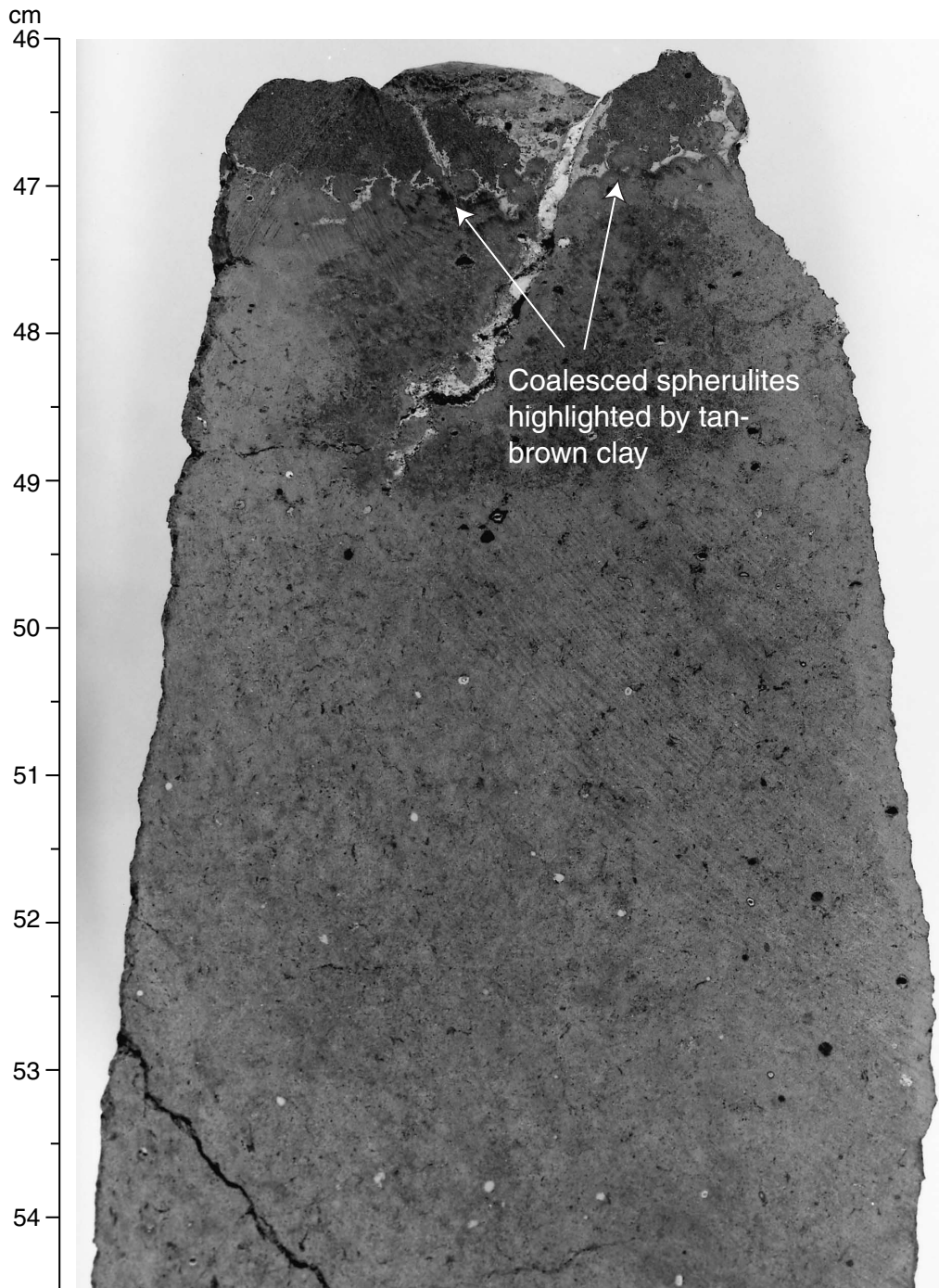


Figure F12. Photograph of interval 187-1159A-6R-2, 63–70 cm, showing a piece of clay-cemented hyaloclastite. The individual glass fragments are partially to completely altered to yellowish brown palagonite.

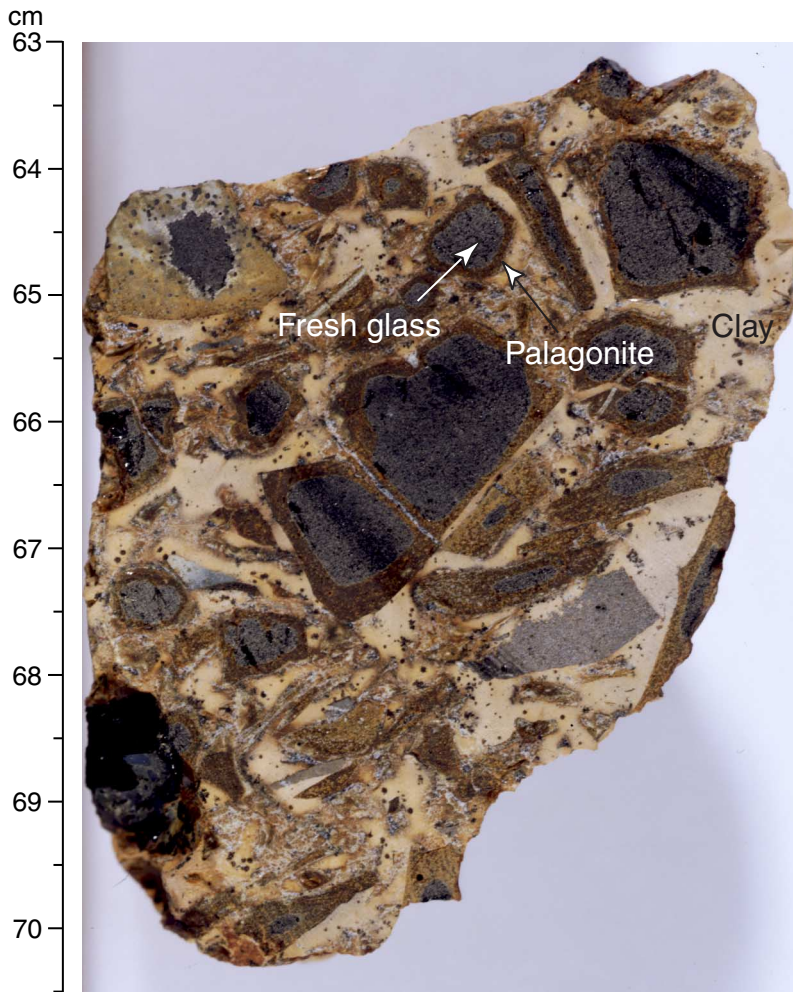


Figure F13. Track chart of the *JOIDES Resolution* single-channel seismic survey line S7. Crosses = 500-shot intervals. Site 1159's location is identical to the prospectus site AAD-2b.

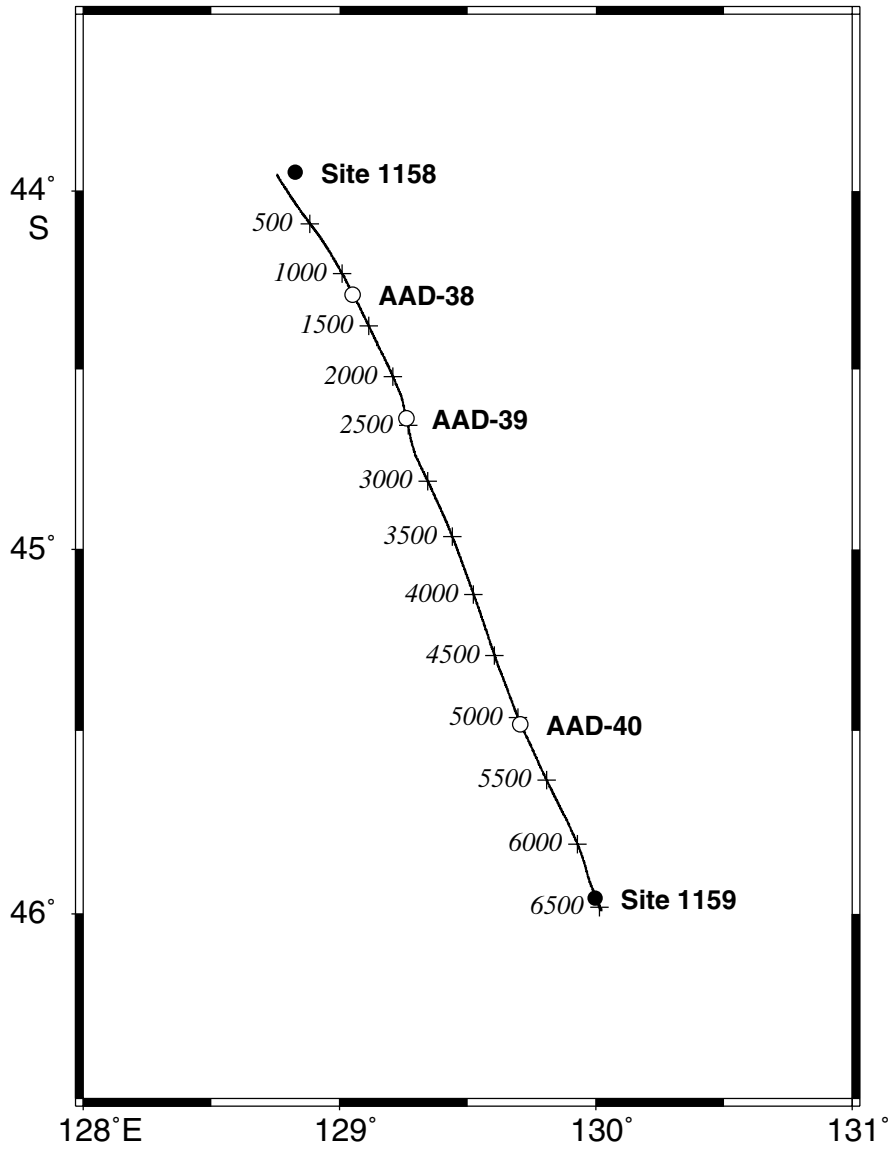


Figure F14. The single-channel seismic profile of line S7 from shotpoints 6270 to 6480. A large arrow marks the position of Site 1159 near shotpoint 6425.

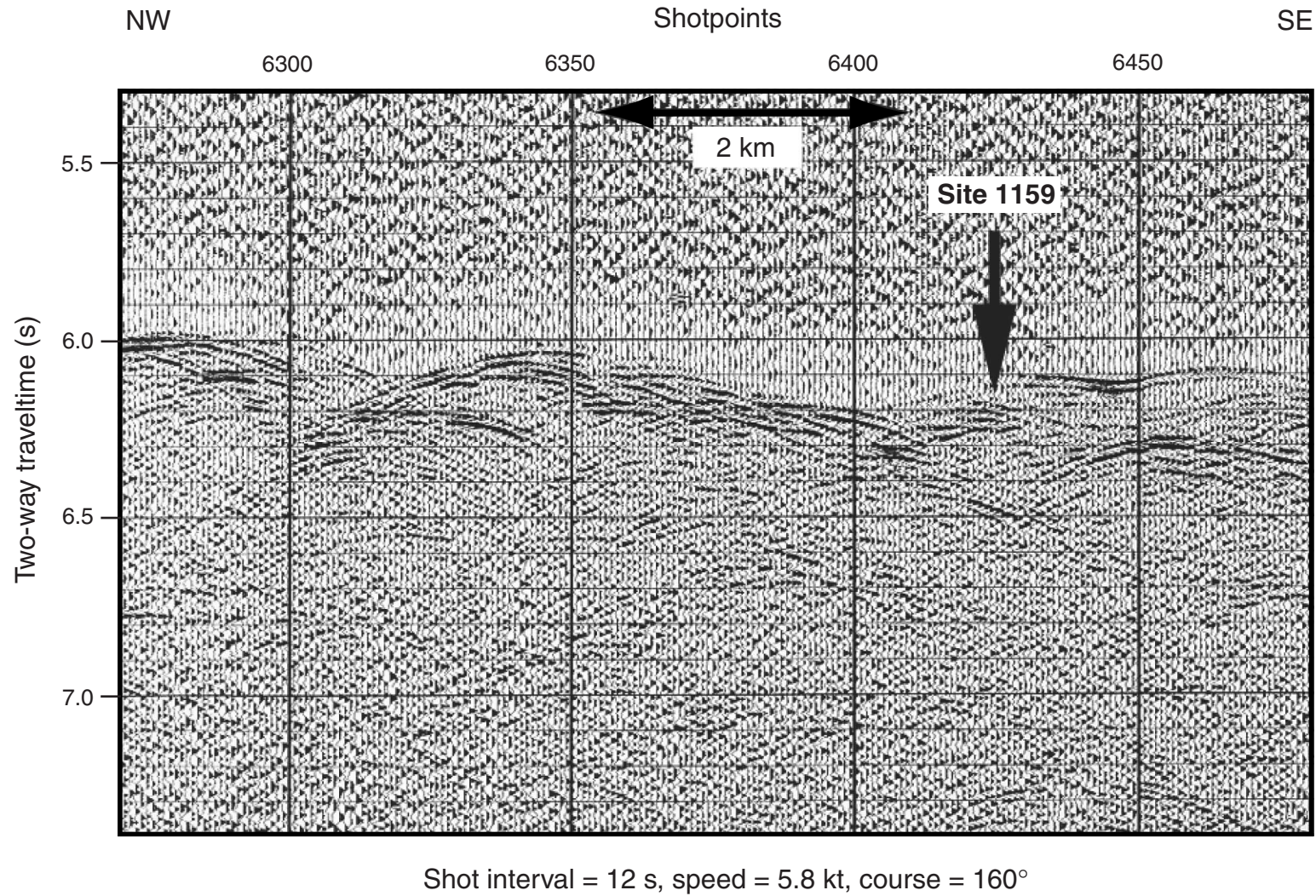


Figure F15. The single-channel seismic profile of line S7 from shotpoints 1025 to 1285. An arrow marks the position of site AAD-38a near shotpoint 1200. The sediment cover extends from 6.79 to 6.94 s in two-way traveltimes, equivalent to 150 m of sediment.

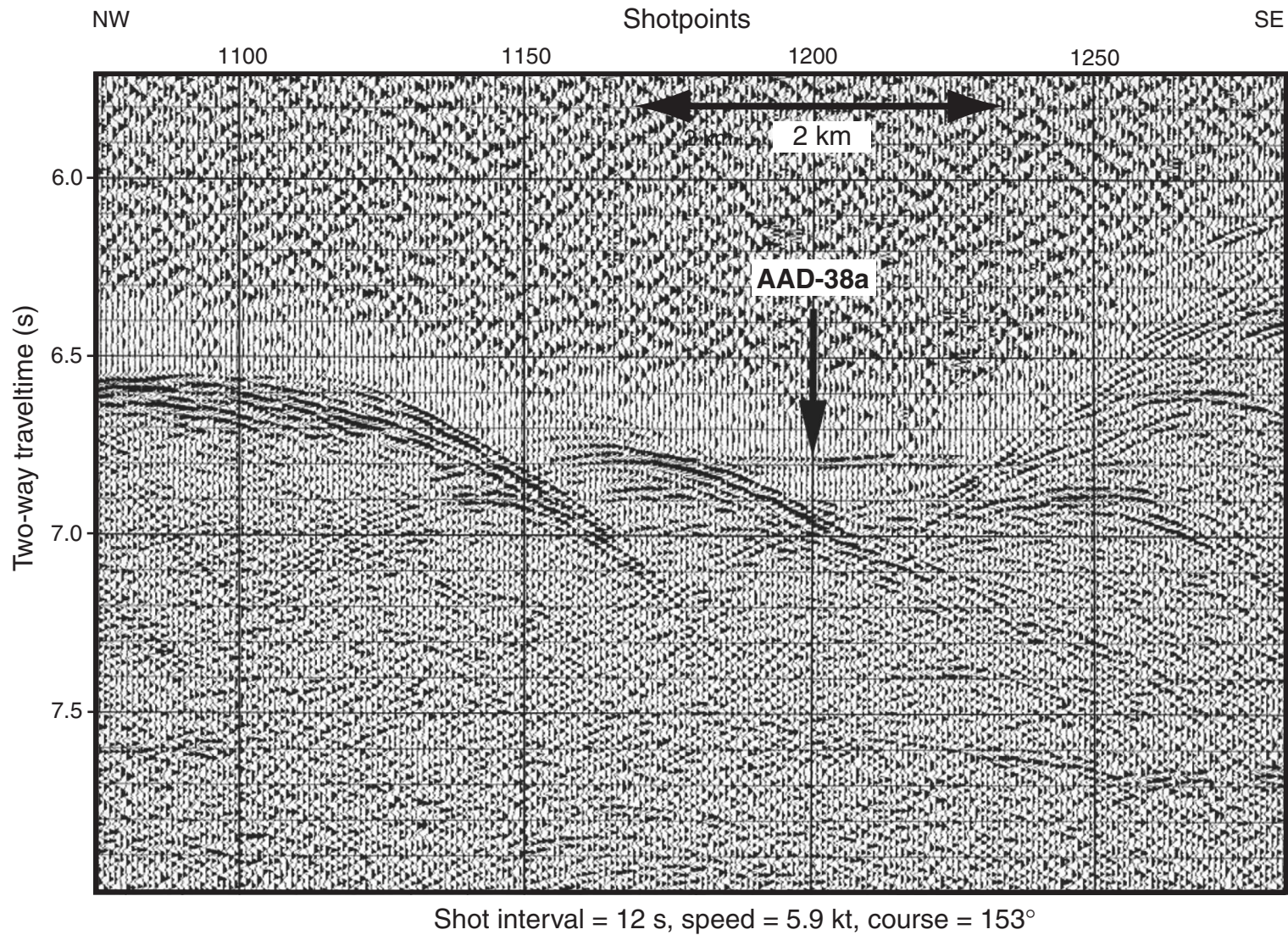


Figure F16. The single-channel seismic profile of line S7 from shotpoints 2110 to 2580. An arrow marks the position of site AAD-39a near shotpoint 2425. The sediment cover extends from 7.47 to 7.75 s in two-way traveltime, equivalent to 280 m of sediment.

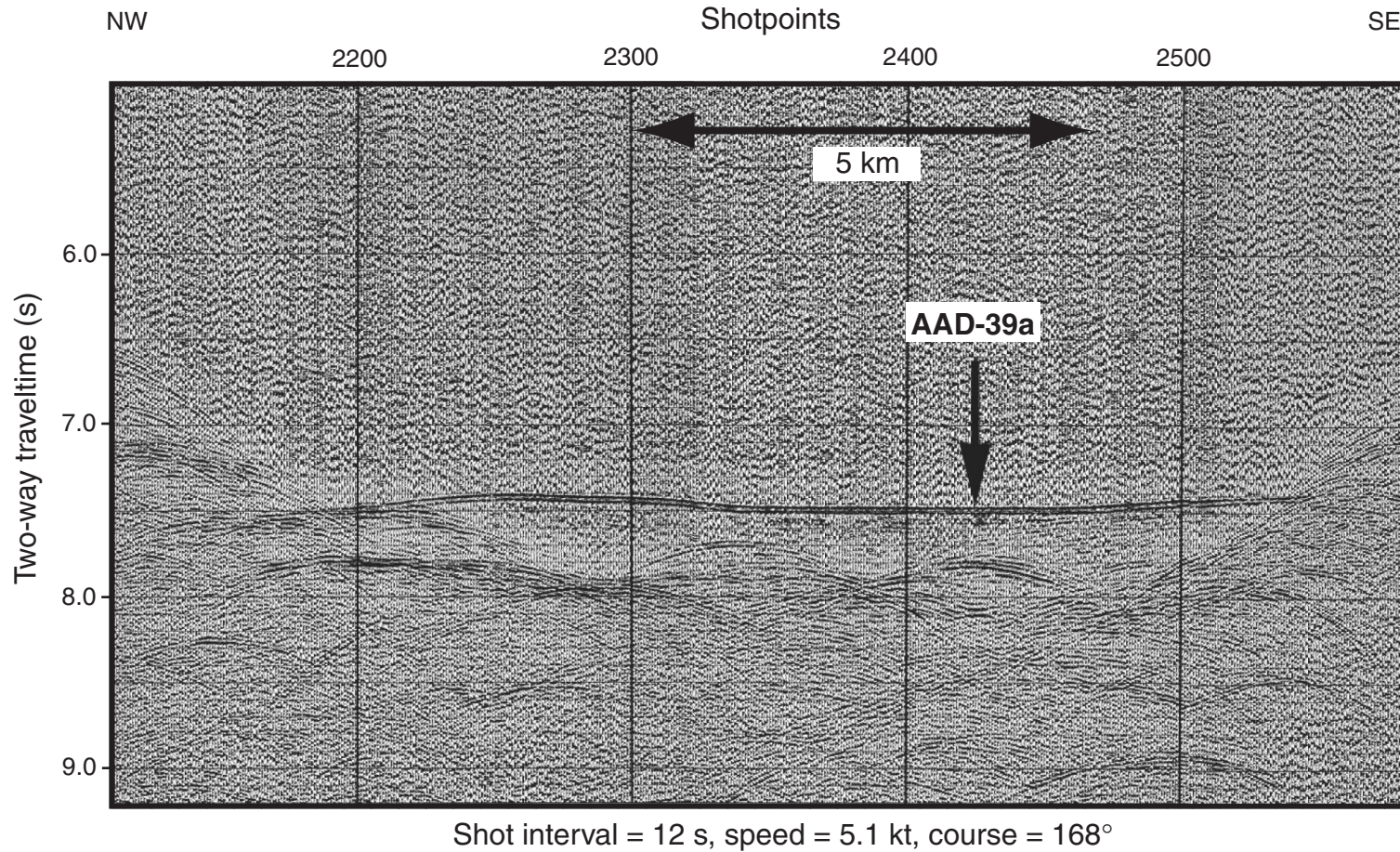


Figure F17. The single-channel seismic profile of line S7 from shotpoints 4935 to 5215. An arrow marks the position of site AAD-40a near shotpoint 5050. The sediment cover extends from 6.30 to 6.58 s in two-way traveltimes, equivalent to 280 m of sediment.

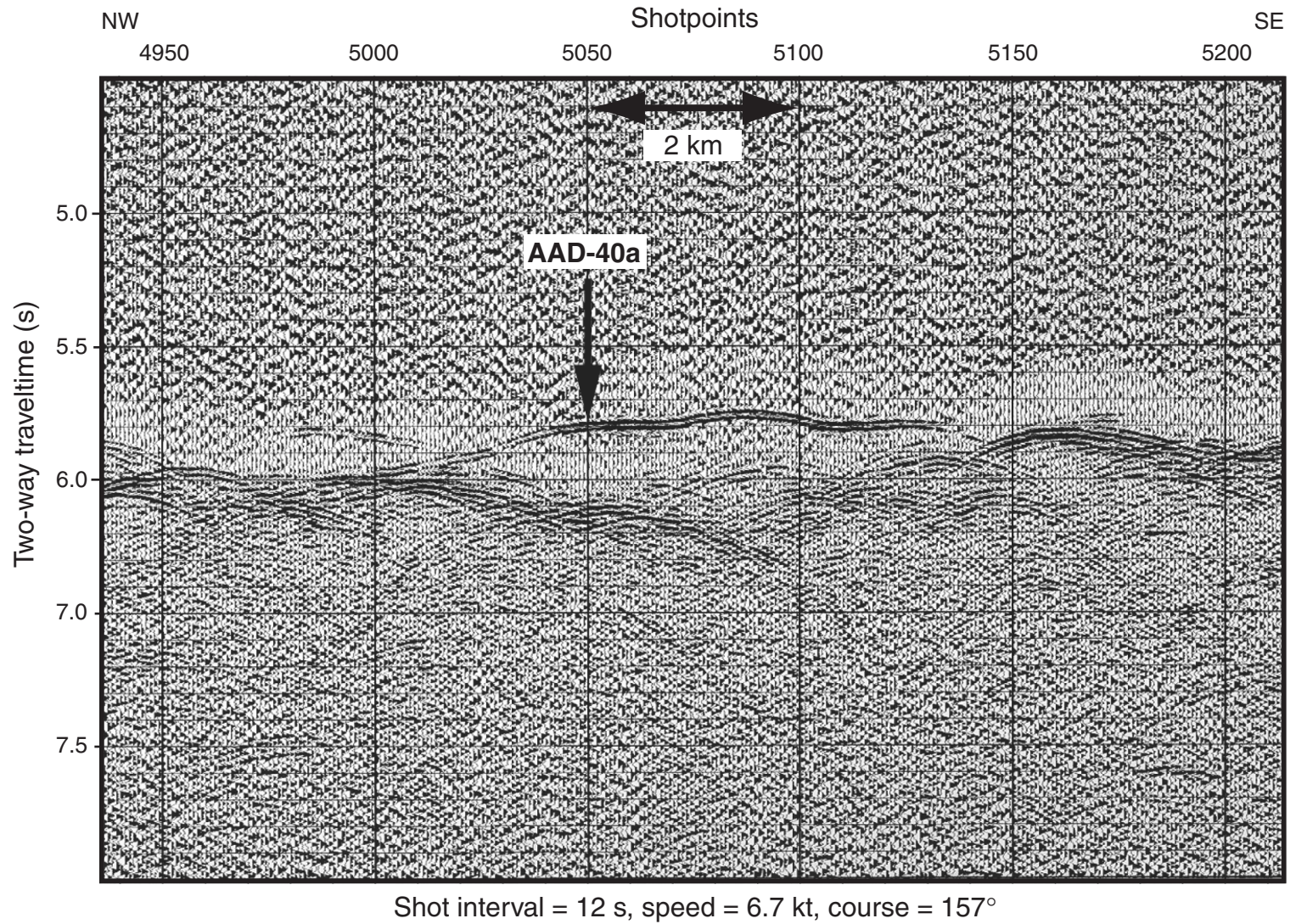


Figure F18. Major element compositions vs. MgO of Site 1159 basalts compared with Southeast Indian Ridge glasses from Zone A Segments A2 and A3 zero-age basalt glass. PRT = propagating rift tip lavas from Segments A2 and A3. Only average X-ray fluorescence or average rerun ICP-AES values are shown.

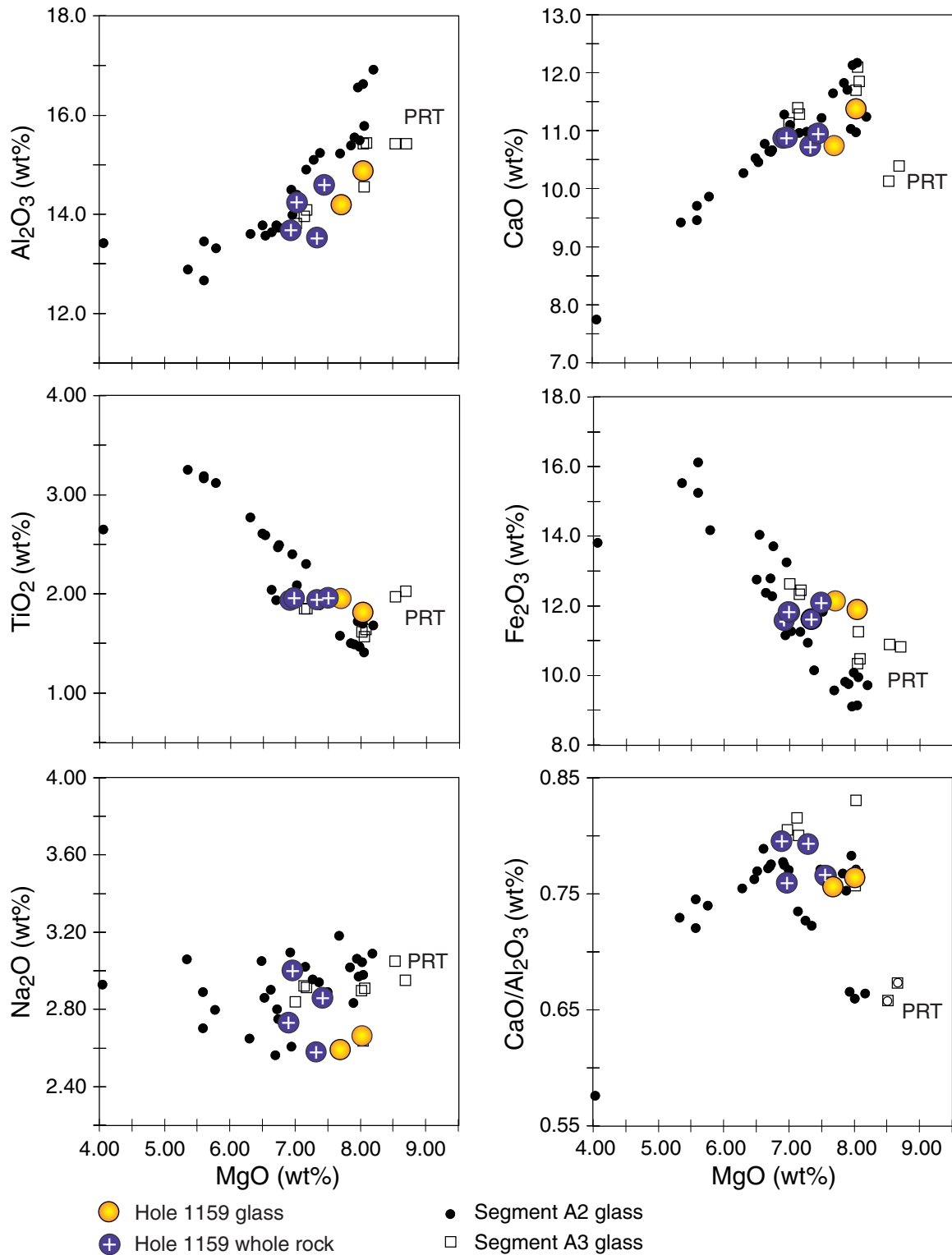


Figure F19. Trace element compositions vs. MgO of Site 1159 basalts. PRT = propagating rift tip lavas from Segments A2 and A3.

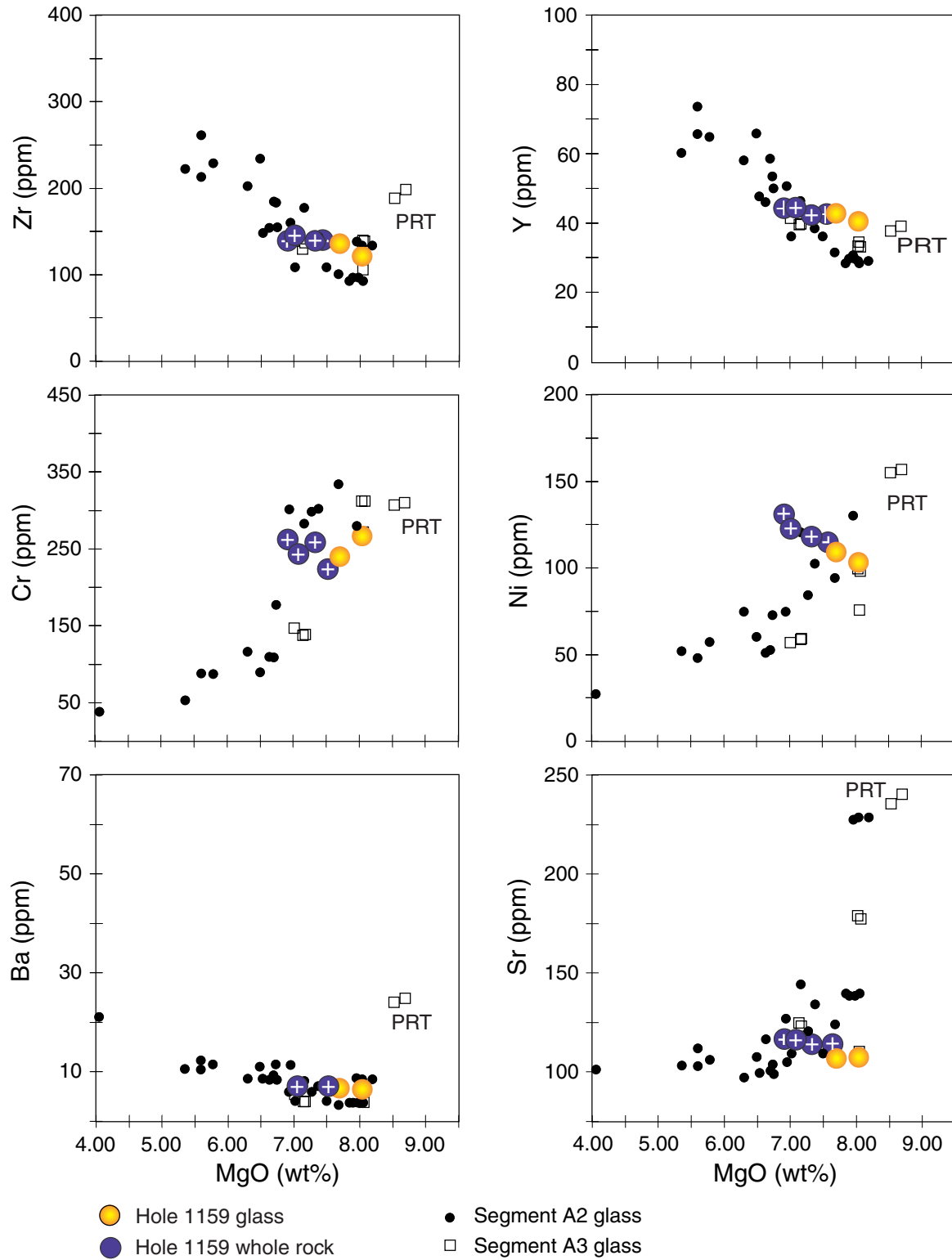


Figure F20. A. Variations of Zr/Ba vs. Ba for Site 1159 basaltic glass and whole-rock samples compared with Indian- and Pacific-type mid-ocean-ridge basalt (MORB) fields defined by zero-age Southeast Indian Ridge (SEIR) lavas dredged between 123°E and 133°E. TP = Transitional Pacific; PRT = propagating rift tip lavas from Segments A2 and A3. **B.** Variations of Na₂O/TiO₂ vs. MgO for Site 1159 basaltic glass and whole-rock samples compared with Indian- and Pacific-type MORB fields defined by zero-age SEIR lavas dredged between 123°E and 133°E. PRT = propagating rift tip lavas from these segments. The dashed line separates Indian- and Pacific-type zero-age SEIR basalt glass.

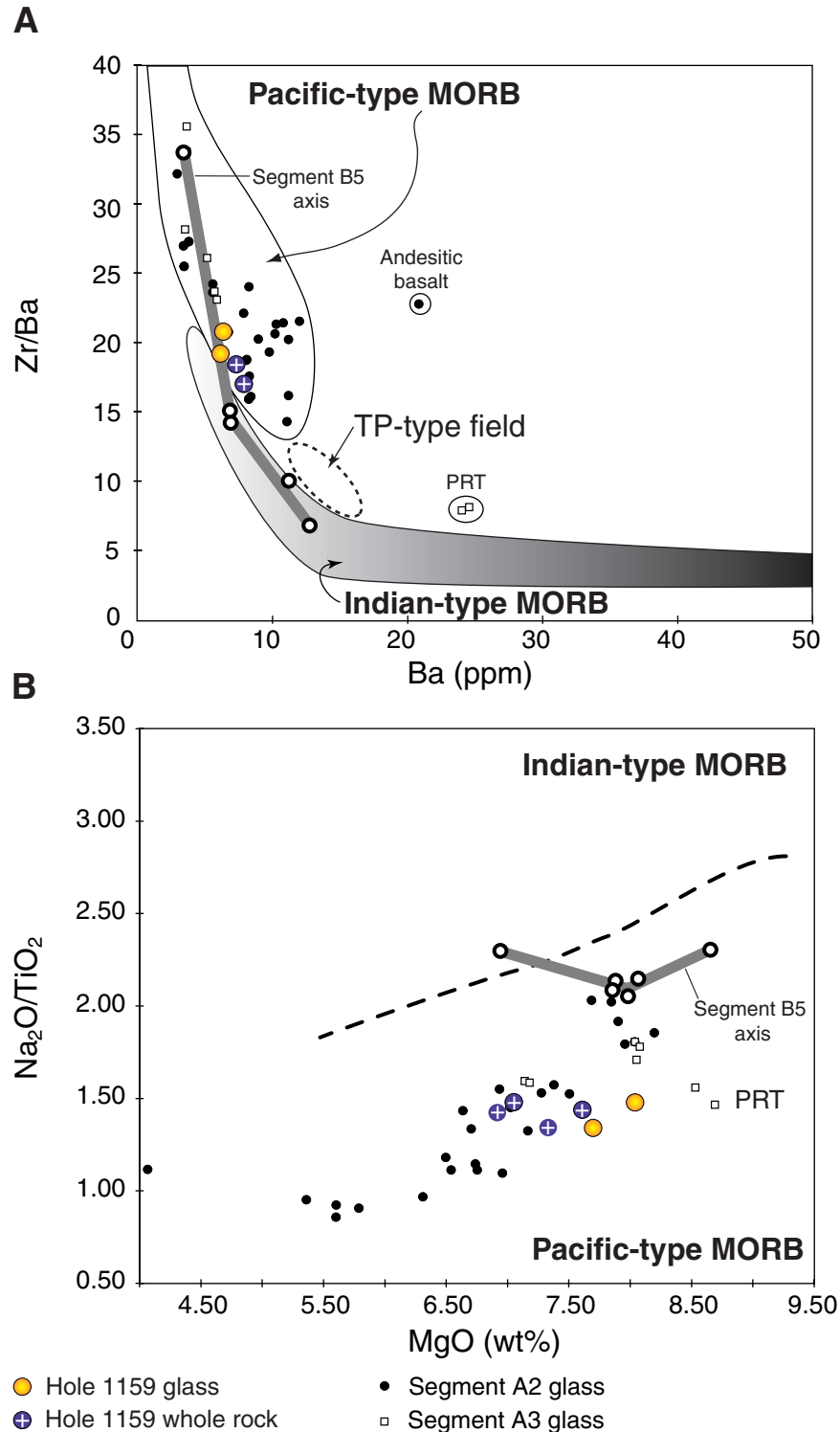


Table T1. Coring summary, Site 1159.

Hole 1159A

Latitude: 45°57.4021'S
 Longitude: 129°59.9940'E
 Time on hole: 2215 hr, 18 Dec 99–2000 hr, 20 Dec 99 (45.75 hr)
 Time on site: 2215 hr, 18 Dec 99–2000 hr, 20 Dec 99 (45.75 hr)
 Seafloor (drill-pipe measurement from rig floor, mbrf): 4515.4
 Distance between rig floor and sea level (m): 11.2
 Water depth (drill-pipe measurement from sea level, m): 4504.2
 Total depth (from rig floor, mbrf): 4688.7
 Total penetration (mbsf): 173.3
 Total length of cored section (m): 27.7
 Total length of drilled intervals (m): 173.3
 Total core recovered (m): 7.96
 Core recovery (%): 28.7
 Total number of cores: 6
 Total number of drilled cores: 1
 Total number of ghost cores: 1

Core	Date (Dec 1999)	Ship local time	Depth (mbsf)		Length (m)		Recovery (%)	Comment
			Top	Bottom	Cored	Recovered		
187-1159A-								
1W	19	1100	0.0	145.6	145.6	4.54	N/A	
2R	19	1350	145.6	148.6	3.0	0.97	32.3	Whirl-Pak
3R	19	1745	148.6	152.8	4.2	1.15	27.4	
4R	19	2225	152.8	157.3	4.5	0.85	18.9	
5R	20	0200	157.3	161.6	4.3	1.88	43.7	
6R	20	0430	161.6	166.7	5.1	1.70	33.3	
7R	20	0755	166.7	173.3	6.6	1.41	21.4	
8G	20	1030	173.3	173.3	0.0	(0.24)	N/A	Ghost core
				Cored:	27.7	7.96	28.7	
				Drilled:	145.6			
				Total:	173.3			

Notes: Parentheses indicate material recovered without additional penetration (not included in recovery calculations). N/A = not applicable.
 This table is also available in [ASCII](#) format.

Table T2. Rock samples incubated for enrichment cultures and prepared for DNA analysis and electron microscope studies and microspheres evaluated for contamination studies.

Core	Depth (mbsf)	Sample type	Enrichment cultures				DNA analysis			SEM/TEM samples	Microspheres [†]		
			Anaerobic	Aerobic	Microcosm*	High pressure	Wash	Centrifuged	Fixed	Air dried	Exterior	Interior	
187-1159A-													
2R	145.6-148.6	Chilled margin	4	1			X			X		Yes	No
3R	148.6-152.8	Chilled margin	9	3	1 Fe/S	X	X			X	X		
6R	161.6-166.7	Breccia	1		1 Mn		X			X	X		
7R	166.7-173.3	Chilled margin				X							
		Seawater							X	X			

Notes: * = microcosm for iron and sulfur (Fe/S) or manganese (Mn) redox cycles; SEM = scanning electron microscope; TEM = transmission electron microscopy; † = contamination test; X = samples prepared on board. This table is also available in [ASCII](#) format.

Table T3. Glass and whole-rock major and trace element compositions of basalts, Hole 1159A.

Hole 1159A										
Core, section:	1W-CC	1W-CC	2R-1	2R-1	2R-1	5R-1	5R-1	5R-1	6R-2	6R-2
Interval (cm):	10-13	10-13	20-24	20-24	20-24	127-131	127-131	127-131	64-70	64-70
Depth (mbsf):	4.47	4.47	145.80	145.80	145.80	158.57	158.57	158.57	163.74	163.74
Piece:	2	2	3	3	3	17	17	17	10	10
Analysis:	ICP	ICP	ICP	XRF	XRF	ICP	XRF	XRF	ICP	ICP
Rock type:	Glass	Glass	Whole rock	Glass	Glass					
Major element (wt%)										
SiO ₂	50.15	50.36	48.56	49.56	50.04	48.69	49.22	49.25	51.20	50.73
TiO ₂	1.92	1.96	1.96	1.92	1.93	1.97	1.90	1.96	1.81	1.81
Al ₂ O ₃	14.15	14.24	14.39	13.62	13.73	14.28	13.56	13.52	14.76	15.00
Fe ₂ O ₃	12.03	12.18	11.82	11.51	11.57	11.89	11.61	11.55	11.81	11.90
MnO	0.19	0.19	0.18	0.17	0.17	0.19	0.17	0.19	0.18	0.20
MgO	7.56	7.83	6.98	6.88	6.94	7.46	7.35	7.30	8.01	8.06
CaO	10.65	10.81	10.85	10.83	10.90	10.85	10.76	10.69	11.36	11.37
Na ₂ O	2.57	2.62	3.02	2.71	2.75	2.77	2.58	2.58	2.53	2.80
K ₂ O	0.09	0.09	0.50	0.36	0.36	0.33	0.24	0.25	0.11	0.11
P ₂ O ₅	0.19	0.19	0.18	0.18	0.18	0.18	0.18	0.18	0.17	0.18
LOI				0.65	0.65		0.31	0.31		
CO ₂										
H ₂ O										
Total:	99.50	100.47	98.45	98.39	99.22	98.61	97.88	97.78	101.94	102.14
Trace element (ppm)										
Nb				5			5			
Zr	137	132	145	138		138	138		115	126
Y	42	44	46	44		45	42		41	40
Sr	106	106	116	116		112	113		105	108
Rb				6			4			
Zn				104			104			
Cu				64			62			
Ni	110	108	121	131		112	118		102	105
Cr	239	240	232	262		227	258		255	277
V				346			356			
Ce				32			35			
Ba	7	7	10			10			6	6
Sc	40	39	39			36			38	42

Notes: CC = core catcher; LOI = loss on ignition. This table is also available in [ASCII](#) format.